Volume 10, Issue 4, 2020, 5843 - 5848 ISSN 2069-5837
Biointerface Research in Applied Chemistry
www.BiointerfaceResearch.com
https://doi.org/10.33263/BRIAC104.843848
Original Research Article Open Access Journal
Received: 20.03.2020 / Revised: 12.04.2020 / Accepted: 14.04.2020 / Published on-line: 18.04.2020

Electrochemical study of anatase TiO_2 in aqueous sodium-ion electrolytes

Kudekallu Shiprath [1], H. Manjunatha [1*], K. Venkata Ratnam [1], S. Janardhan [1], A. Ratnamala [1], R. Venkata Nadh [1], S. Ramesh [2], K. Chandra Babu Naidu [2]
[1] Department of Chemistry, GITAM School of Science, GITAM (Deemed to be University), Bengaluru, Karantaka, India
[2]Department of Physics, GITAM School of Science, GITAM (Deemed to be University), Bengaluru, Karantaka, India
*Corresponding author email address: ***hanumanjunath80@gmail.com*** | Scopus ID 57188956297

ABSTRACT
In this paper, a basic electro-analytical study on the behavior of anatase TiO_2 in aqueous NaOH has been presented using cyclic voltammetry technique (CV). The study has explored the possibility of using TiO_2 as anode material for ARSBs in presence of 5 M NaOH aqueous electrolyte. CV profiles show that anatase TiO_2 exhibits reversible sodium ion insertion/de-insertion reactions. CV studies of TiO_2 anode in aqueous sodium electrolytes at different scan rate shows that the Na^+ ion insertion reaction at the electrode is diffusion controlled with a resistive behavior. Proton insertion from aqueous sodium electrolytes into TiO_2 cannot be ruled out. To confirm the ion inserted and de-inserted, CV studies are done at different concentration of NaOH and it is found that at lower concentrations of NaOH, proton insertion process competes with Na^+ ion insertion process and as the concentration increases, the Na^+ ion insertion process becomes the predominant electrode reaction making it suitable anode materials for aqueous sodium batteries in 5 M NaOH.
Keywords: *Anatase TiO_2;Aqueous sodium-ion batteries; electrochemical study; Cyclic voltammetry (CV).*

1. INTRODUCTION

Rechargeable batteries play a significant role in harvesting and storing renewable, environmentally friendly energy resources like wind and solar energy which are inherently intermittent. The development of advanced energy storage technology is of great importance in harvesting these energy resources to address the increasing global concern of energy crisis and environmental protection [1].

At present, lithium based batteries represents the most advanced battery technology owing to their high energy density and high standard voltage. However, their applications are mostly dominated by portable electronic devices and attract less attention of researchers for high end applications such as gird-scale or stationary energy storage systems [2-4]. This is due to the fact that lithium is expensive and its reserves are limited on earth. In contrast to lithium, sodium offers several advantages like suitable redox potential (E = -2.71 V vs. SHE), a value close to that of lithium (E = -3.05 V vs. SHE), very abundant and cheap. Sodium ion batteries [NIBs] with non-aqueous electrolytes have been investigated as good alternatives to their lithium counterparts [5-9]. NIBs with aqueous electrolytes [ARSBs] are particularly beneficial as the electrolytes can be prepared with cheap materials like water and simple salts such as NaOH, NaCl, Na_2SO_4, $NaNO_3$ etc.

In addition, aqueous electrolytes possess more ionic conductivity, safety, environmentally friendly and can deliver higher power densities than non-aqueous electrolytes. Several materials have been studied as anodes in ARSBs like nasicon type $NaTi_2(PO_4)_3$ [10-12], Vanadium based compounds [13], carbonyl based organic compounds [14], Prussian blue analogs and their derivatives[15]. TiO_2 is an inexpensive, exceptionally stable, non-toxic and abundant [16] electrode material. In nature, TiO_2 exists in different polymorphs such as rutile (tetragonal), brookite (orthorhombic) and anatase (tetragonal) [17-21]. Most thermodynamically stable and common phases of TiO_2 are rutile and anatase forms. The ability of anatase TiO_2 to intercalate reversibly foreign ions such as H^+, Li^+ and Na^+ in its host structure makes it an excellent candidate for rechargeable lithium and sodium ion batteries in addition to its high stability and semiconducting properties.

The electrochemical behavior of TiO_2 has been widely studied in non-aqueous sodium ion electrolytes [17-21]. However, the information available on the electrochemical study of anatase TiO_2 in aqueous electrolytes is very less. Lyon and Hupp [22, 23] showed that TiO_2 undergoes irreversible proton (H^+) insertion from aqueous H_2SO_4 and NaOH solutions. This mechanism was also supported by electrochemical quartz crystal microbalance (EQCM) measurements. Later, the use of anatase TiO_2 as an anode in ARSBs in presence of 1 M NaOH and 1 M NaCl was reported [22]. In this work, TiO_2 nanotube electrodes are grown directly on a current collector using a fixed voltage or a voltage ramp. A study of their ability to accommodate Na^+ ion has been presented as a function of the potential used for the electrochemical growth of the nanotubes and the temperature used for their annealing. The study proved that anatase undergoes reversible sodium insertion/de-insertion in 1 M NaOH and 1 M NaCl. However, the information was very brief and a detailed cyclic voltammetry study of the electrochemical behavior of anatase TiO_2 in aqueous different aqueous sodium electrolytes is not reported to the best of our knowledge. Such knowledge of the electrochemical behavior of TiO_2 is necessary in order to use it as an anode material in aqueous rechargeable sodium ion batteries.

In modern electro-analytical chemistry, cyclic voltammetry (CV) is the basic and first tool of choice to analyze the reversibility of an electrochemical system[24]. In this method, a cyclic linear potential ramp is imposed on an electrode and the resulting current response of the electrode system is recorded. By analyzing the CV profiles, one can get the first information on kinetics, mass transport and reversibility of an electrode system. A redox reaction involving both an oxidant (O) & a reductant (R) rapidly exchanging electrons with the electrode is called an electrochemical reversible redox system. In CV technique, an ideal

reversible redox system involving single electron transfer must satisfy certain characteristics at equilibrium. They are as follows.

a. The oxidation and reduction peak potential separation i. e. $\Delta E_p = 0.058/n$ V at all scan rates at 25 °C.

b. The ratio of the cathodic to anodic peak currents must be unity i. e. $i_{pa}/i_{pc} = 1$

c. The peak currents should be proportional to the square root of scan rate i. e $i_p \alpha v^{1/2}$.

The peak current (i_p) is related to diffusion coefficient by Randles - Sevick equation as shown below

$$i_p = 0.446nF\,(nF/RT)^{1/2}C^*\,v^{1/2}AD^{1/2} \quad (1)$$

In practice, the CV profiles very rarely satisfy the above conditions for reversibility of a system. This is due to the fact that the rate of reaction at the electrode-electrolyte interface is affected by slow electron transfer kinetics which arises from the solution resistance and also resistance offered by solid state reaction. These factors which lead to polarization of the electrode are more pronounced in redox systems with lithium/sodium intercalation/de-intercalation chemistry and understanding their reaction kinetics is highly complicated than solution based systems. This is due to the fact that the electrode material itself takes part in the reaction with the movement of lithium/sodium ions in and out of electrode's active material.

2. MATERIALS AND METHODS

2.1. Chemicals and characterization.

Crystal structure of the anode material, TiO_2 was confirmed by powder XRD using Bruker's X-ray powder diffractometer with Cu-Kα radiation as source (λ = 1.5418 Å).Anatase TiO_2 (99.5%) powder was purchased from Sigma-Aldrich and used as received.

The other chemicals used in this study were of analytical grade from Sigma–Aldrich and used as received.Stainless steel (SS) was used as a current collector. The working electrode was prepared by sand blasting a SS mesh to remove the surface oxide layer and generate a rough surface. Then the SS mesh of 2.23 cm^2 geometric surface areas with a tag for electrical connection was etched in dil. HNO_3, cleaned with detergent, washed with water, rinsed with acetone, dried and weighed. TiO_2, acetylene black and polytetrafluoroethylene (PTFE) were taken in the weight ratio of 70:20:10 in an agate mortar and grounded. The acetylene black enhances the electrical conductivity of the TiO_2 active materials and PTFE acts as binder.

Few drops of N-methyl-2-pyrrolidinone (NMP) were added to the above mixture to make slurry. The slurry was coated on to a previously weighed SS mesh and dried at 60 °C overnight under vacuum. The active material loading was 15 mg cm^{-2}. Cyclic voltammetry measurements were done in a glass cell of capacity 25 ml using NaOH, $NaNO_3$ and Na_2SO_4 aqueous solutions as electrolytes. A Platinum foil and a saturated calomel electrode (SCE) served as counter electrode and the reference electrode respectively. All the experiments were performed at room temperature (25 ˚C) and the potential values given against SCE. Biologic's potentiostat-galvanostat electrochemical workstation, Model VSP, France was used for all electrochemical studies.

3. RESULTS

XRD is a useful tool to confirm the structure of any crystalline material [25]. Crystalline structure of TiO_2 sample was confirmed by powder X-Ray Diffraction studies and is as shown in Fig.1. From the figure, it is clear that the sample TiO_2 has an ordered anatase phase with all the diffraction peaks well indexed with tetragonal crystal structure belonging to *$I4_1/amd$* space group. No peaks belonging to any impurities were detected in the XRD and the pattern obtained is in good agreement with that reported in literature for TiO_2 [10, 15].

3.1. Cyclic voltammetry study of TiO_2 in aqueous solutions.

The CV profile of SS mesh current collector used for the preparation of TiO_2 working electrode in 5 M NaOH is as shown in Fig. 2a. It is very clear that the peak current which corresponds to the evolution of oxygen is observed outside the potential window used for recording the CV profile of TiO_2 as shown in Fig. 2b. Also, the peak current which corresponds to the evolution of hydrogen was observed within the stable potential window used for recording the CV profile of TiO_2. This indicates that the 5 M NaOH provides stable potential window for Na^+ insertion and de-insertion in TiO_2.

The CV profile of TiO_2 shows a reduction peak at -0.27 V and its corresponding anodic peak is at + 0.003 V. A large potential gap of 0.273 V was observed between oxidation and reduction peaks suggesting that the kinetics of electron transfer process is very slow in aqueous 5 M NaOH. When subjected to continuous cycling (10 cycles) in the potential range of -0.50 V to +0.20 V at a scan rate of 1 mV s^{-1}, TiO_2 shows some changes in its CV profile as shown in Fig. 2(C). The cathodic and anodic peak currents decreased up to 8^{th} cycle and then tend to stabilize, suggesting that TiO_2 could be reversibly reduced/oxidized over a number of cycles.

3.2. Effect of scan rate.

To study the reversibility of TiO_2 anode material in 5 M NaOH, cyclic voltammograms were recorded at different scan rates varying between 0 mV $s^{-1}$to 5 mV s^{-1} and are as shown in Fig. 3(A). From the figure it is found that the peak-to-peak separation(ΔE_p) increases with an increasing scan rate, a linear dependence of current with applied potential (*I-E*) was found during an initial increase in current and all the CV profiles overlap irrespective of scan rate atthe beginning of charging and discharging. The last two observations suggest that the initialcurrent is a linear function of the potential. A plot of anodic and cathodic peak currents vs. square root of scan rate is as shown in Fig. 3(B). A straight line between i_p and $v^{1/2}$ was observed over the scan rates at which the CV profiles were recorded.

As discussed in the introduction, this forms one of the characteristics for reversibility of reversible system i.e. $i_p \alpha v^{1/2}$ relationship (characteristic c). The lowest scan rate applied to get the real separation between anodic and cathodic peaks in this study was 100 μV s^{-1} and the ΔE_p was found to be about 0.159 V which is large to compared to the theoretical value of 0.059 V for an one electron transfer redox system to be reversible (characteristic a).

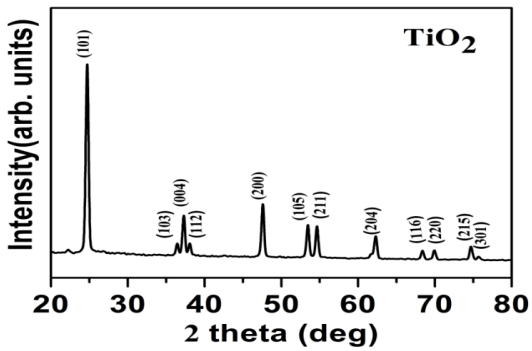

Figure 1. X-ray diffraction pattern of TiO_2

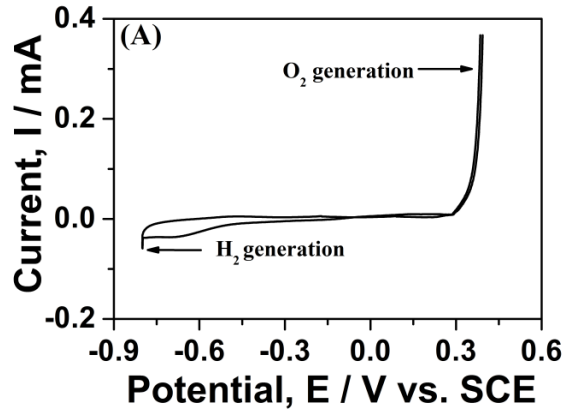

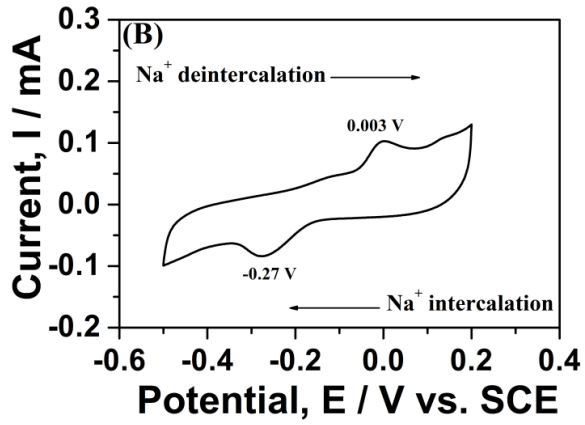

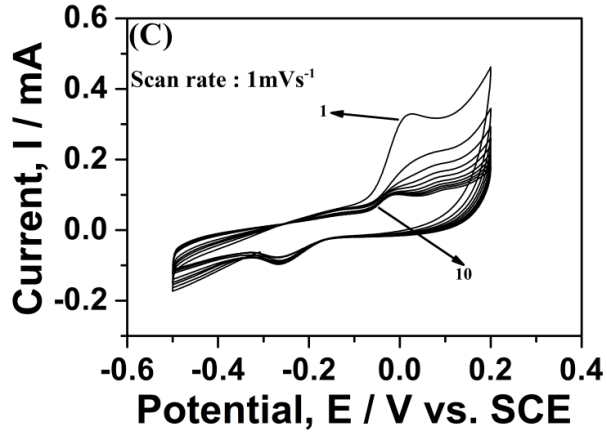

Figure 2. Cyclic voltammogram of, (A) Stainless steel mesh (SS) in 5 M NaOH aqueous solution (scan rate; 1 mV s^{-1}), (B) TiO_2 electrode in 5 M NaOH aqueous solution (scan rate; 1mV s^{-1}), (C) ten-cycle on TiO_2 electrode in 5 M NaOH aqueous solution.

This large potential gap can be assigned to the slow electron transfer kinetics at TiO_2 in 5 M NaOH solution [16]. In order to satisfy the characteristic b, the anodic and cathodic peak currents must have the same magnitude. However, Fig. 3b shows that this condition also is not satisfied at all scan rates, i.e. $i_{pc}/i_{pa} \neq 1$. This could be due to the fact that sodium interaction and de-intercalation into/from TiO_2 follows different mechanism during charge and discharge. Na^+ ions are most likely to be transported through various regions such as anatase TiO_2, Ti_2O_3, sodium peroxide, metallic sodium and amorphous sodium titanate Ti_2O and TiO [22, 23,26]. It is also reported by Manickan et. al. [27] that, in addition to the formation of reversible Li_xTiO_2 , Ti_2O_3, Ti_2O and TiO compounds are irreversibly formed during the electro-reduction of TiO_2 in aqueous solution. These titanium oxide compounds are not formed in non-aqueous cells and may be related to proton intercalation. This difference in the electrochemical environment for Na^+ transport may account for the difference in the magnitude of the peak currents at all the scan rates. Thus we conclude that the characteristic b need not be upheld for TiO_2 system owing to the fact that the integrated area under the cathodic and anodic scans is almost equal (i.e. the same capacities of about 60 mAh g^{-1} for charging and discharging). From the above discussion, it is understood that TiO_2 shows a reversible reaction with a resistive behavior similar to the work reported in non-aqueous electrolytes [23].

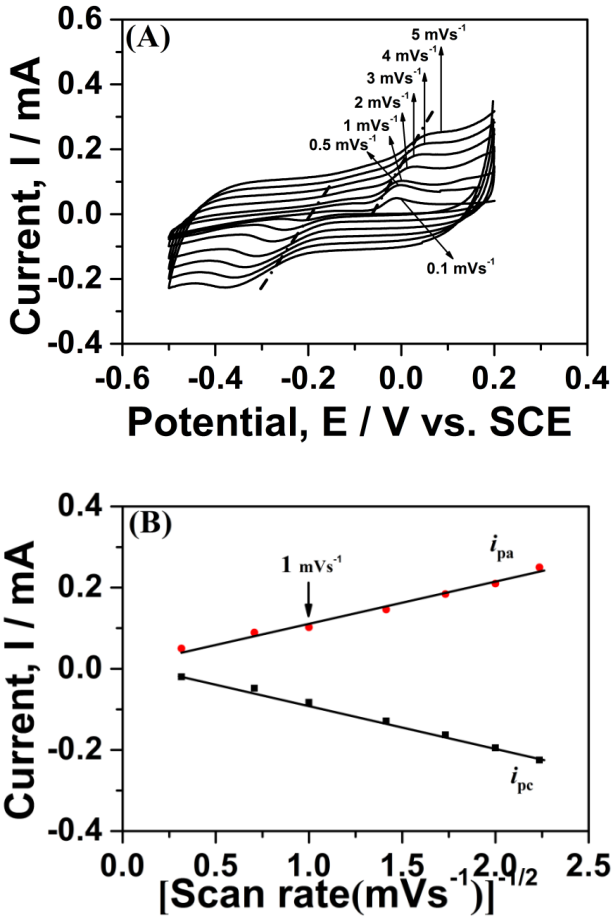

Figure 3. (A) Cyclic voltammograms of TiO_2 recorded in 5 M NaOH aqueous electrolyte at various scan rates. (B) The relation between the peak current density and square root of scan rate, of TiO_2 in aqueous 5 M NaOH solution.

3.3. Identification of cation.

In aqueous electrolytes, Na^+ ion insertion/de-insertion reactions are complicated by the interference of proton insertion reactions. In this concern, identification of the cation being inserted into the TiO_2 anode material becomes important. It is interesting to identify the cation de-intercalated/intercalated from/to TiO_2 upon the redox reaction of Ti^{3+}/Ti^{4+} couple. The electrochemical de-sodiation and sodiation reactions havebeen mentioned for TiO_2 in

aqueous electrolytes [22]. However, a detailed CV study is not available. The reactions for the redox peaks of TiO_2 in Fig. 2a can be written as follows

$$\text{Oxidation:} \quad Na_xTiO_2 \rightarrow xNa^+ + TiO_2$$
$$\text{Reduction:} \quad xNa^+ + TiO_2 \rightarrow Na_xTiO_2$$

The formal potential of a redox reaction depends on the concentration of the active species i.e. sodium ion (a_{Na+}) in accordance with the following Nernst equation (1),

$$E_f = E^\circ + 0.059 \log a_{Na+} \quad \text{----------} \quad (1)$$

In other words, the formal potential, E_f of the redox reaction of TiO_2 in the NaOH aqueous solutions should be directly proportional to the logarithm of the sodium ion activity. The formal potential (E_f) can be calculated from the de-sodiated/ sodiated peak potentials of CV curves recorded at different concentrations of NaOH using the following equation,

$$E_f = E_{pa} + E_{pc}/2$$

The cyclic voltammetry curves of TiO_2 electrode were recorded in various concentrations of NaOH viz, 0.5, 1, 2, 3, 4 and finally in 5 M NaOH and are as shown in Fig. 4(A). From the figure, the CV profile obtained in 0.5 M NaOH show an oxidation peak at 0.150 V and a reduction peak at -0.110 V with a formal potential of -0.02 V.

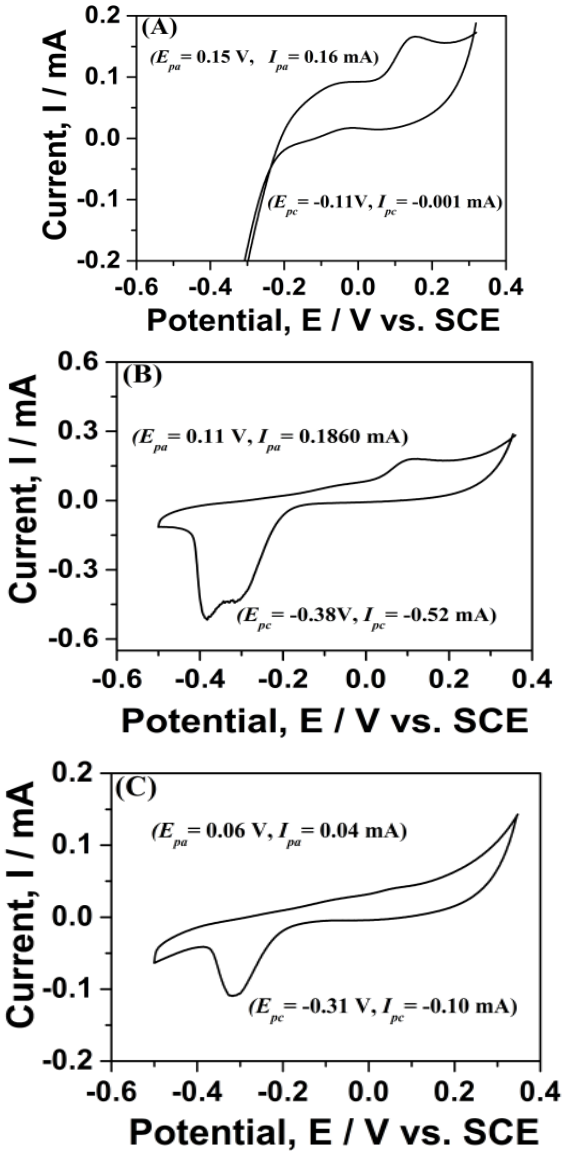

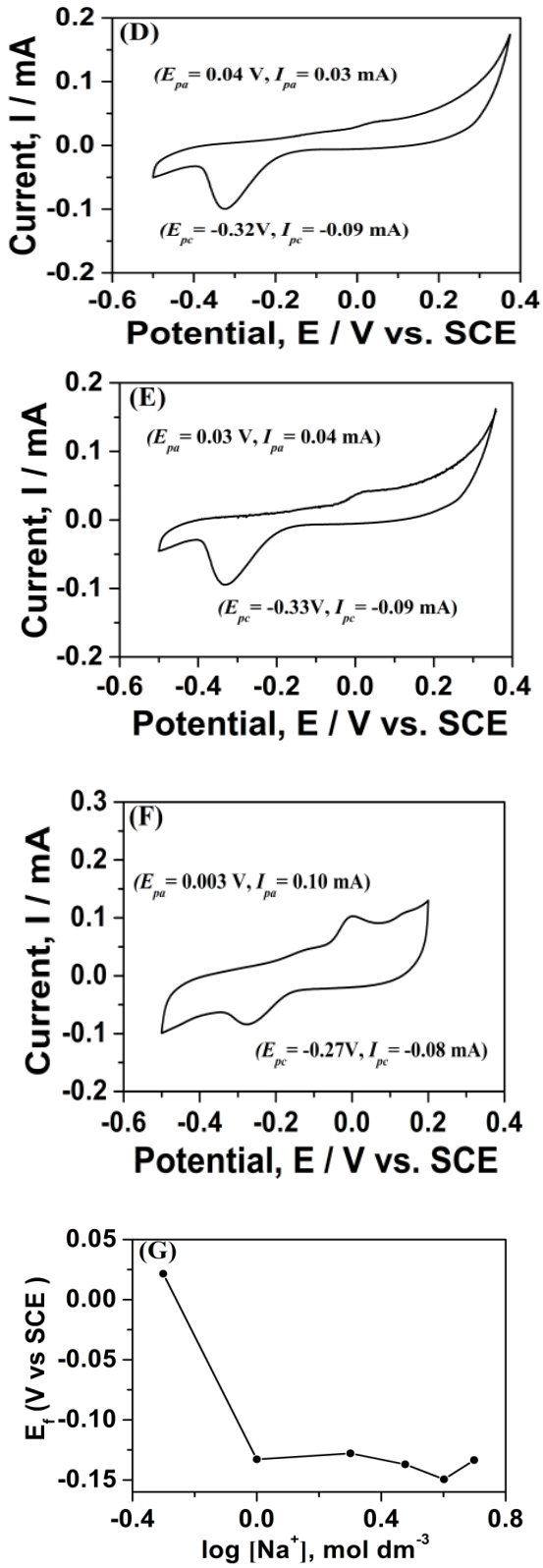

Figure 4. Cyclic voltammograms of TiO_2 in different concentration of, (A) 0.5 M NaOH, (B) 1 M NaOH, (C) 2 M NaOH, (D) 3 M NaOH, (E) 4 M NaOH, (F) 5 M NaOH and (G) Plot of E_f vs. log [Na^+].

The anodic and cathodic peak currents are also low. However, as the concentration of the electrolyte increases to 1 M, a significant change in the CV profile was observed. Both the cathodic and anodic currents increased with an increased peak potential separation. The cathodic peak is found to be having two submerged peaks. We believe that the two peaks represent two different intercalation reactions taking place at TiO_2 i.e., sodium ion and proton intercalation. This supports the previous reports by Lyon

and Hupp [28, 29] that TiO_2 undergoes irreversible proton insertion in aqueous NaOH. As the concentration of the electrolyte increased further from 1 M to 2 and 3 M, the two submerged cathodic peaks coalesce and a single peak appears during intercalation. In addition to this, a decrease in the CV peak currents, peak potential separation and formal potential values were also observed at these higher concentrations of electrolyte. The formal potential value was expected to increase in order to support Na^+ ion insertion/de-insertion rather than proton insertion mechansim. However, the decrease observed can be explained as follows.

Fig. 4(B) shows the relationship between the formal potential, E_f and the logarithm of concentration of sodium ions for different concentrations of NaOH to identify the cation being inserted/extracted to/from TiO_2. It is observed that the shapes of the CV curves obtained in various concentrations of NaOH are not similar and do never represent a single redox reaction taking place at TiO_2 electrode. The CV profiles suggest that proton insertion/de-insertion reaction may be coupled with sodium insertion/de-insertion reaction particularly at lower concentrations of NaOH.

3.4. Effect of different electrolyte.

Fig. 5 shows the cyclic voltammogram of TiO_2 anode material recorded in different sodium electrolytes. From the figure, the following observations can be made: In 5 M $NaNO_3$ and Sat. Na_2SO_4, the CV profile of TiO_2 exhibits only one cathodic peak at -0.15 V. The peak potentials of these two peaks coincide with each other and there are no peaks appeared on CV curve during discharge. This indicates that TiO_2 undergoes irreversible proton insertion from these aqueous electrolytes and cannot be used as anode material in ARSBs in presence of 5 M $NaNO_3$ and sat. Na_2SO_4 electrolytes.

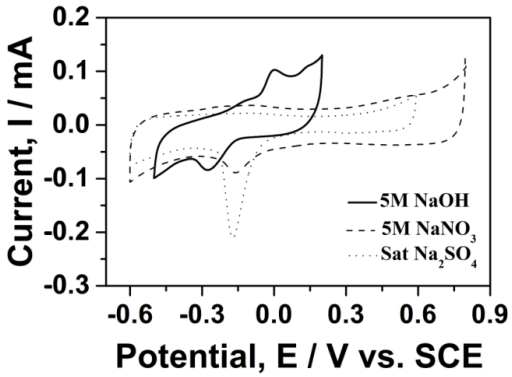

Figure 5. Cyclic voltammograms of TiO_2 in different aqueous electrolytes as indicated in the figure. Scan rate; 1 mV s^{-1}.

However, in 5 M NaOH aqueous electrolyte, two clear and distinct peaks appear during discharge and charge. The oxidation peak appeared at 0.01 V and the reduction peak at -0.15 V vs. SCE suggesting Na^+ ion de-insertion and insertion from the 5 M NaOH respectively. Also the anodic and cathodic peaks tended to shift in negative direction with reduced cathodic peak current indicating the reduced interference or absence of proton insertion kinetic at TiO_2 in 5 M NaOH.

4. CONCLUSIONS

Cyclic voltammetry technique has been used successfully to study the electrochemical behavior of TiO_2 in aqueous sodium electrolytes. The CV studies of TiO_2 show that it undergoes a partially reversible sodium insertion/de-insertion reaction mechanism in aqueous NaOH electrolyte with a resistive behavior. At a lower concentration of sodium ions, TiO_2 was found to undergo proton insertion/de-insertion reaction. However, at higher concentrations, sodium insertion becomes the dominating process taking place at electrode through the interference from proton insertion/de-insertion process cannot be ruled out. Electrochemical sodium ion insertion/de-insertion in TiO_2 from aqueous electrolyte has been proved by using CV technique.

5. REFERENCES

1. Turgut M. G. Review of electrical energy storage technologies, materials and systems: challenges and prospects for large-scale grid storage, *Energy Environ. Sci.* **2018**, 11, 2696—2767, https://doi.org/10.1039/C8EE01419A
2. Prasant Kumar, N: Yang, L: Brehm, W: Adelhelm, P. From Lithium-Ion to Sodium-Ion Batteries: Advantages, Challenges, and Surprises. *Angew. Chem. Int. Ed*. **2018**, 57, 102 – 120, https://doi.org/10.1002/anie.201703772
3. Neha, C: Bharti, N: Shailendra, S. Recent Advances in Non-Flammable Electrolytes for Safer Lithium-Ion Batteries. *Batteries*, **2019**, 5, 19, https://doi.org/10.3390/batteries5010019.
4. Zhu, M: Wu, J: Wang, Y: Song, M: Long, L: Siyal, S.H: Yang, X: Sui, G. Recent advances in gel polymer electrolyte for high-performance lithium batteries. *Journal of Energy Chemistry*, **2019**, 37,126-142, https://doi.org/10.1016/j.jechem.2018.12.013
5. Delmas, C. Sodium and Sodium-Ion Batteries: 50 Years of Research, *Adv. Energy Mater.* **2018**, 1703137. https://doi.org/10.1002/aenm.201703137
6. Rojo, T: Hu, Y-S: Forsyth, M: Li, X. Sodium-Ion Batteries. *Adv. Energy Mater.* **2018**, 8, 1800880, https://DOI: 10.1002/aenm.201800880
7. Pu, X: Wang, H: Zhao, D: Yang, H: Ai, X: Cao, S: Chen, Z: Cao, Y. Recent Progress in Rechargeable Sodium-Ion Batteries: toward High-Power Applications. *Small* **2019**, 1805427, https://doi.org/10.1002/smll.201805427
8. Yang Xu, Y: Zhou, M: Lei, Y. Organic materials for rechargeable sodium-ion batteries, *MaterialsToday*, **2018**, 21, 60-78, https://doi.org/10.1016/j.mattod.2017.07.005
9. Fang, Y: Xiao, L: Chen, Z: Ai, X: Cao, Y: Yang, H. Recent Advances in Sodium-Ion Battery Materials,. *Electrochemical Energy Reviews*. 2018,1, 294–323. https://doi.org/10.1007/s41918-018-0008-x
10. Delmas, C.; Cherkaoui, F.; Nadiri, A.; Hagenmuller, P. A nasicon-type phase as intercalation electrode: NaTi2(PO4)3. *Materials Research Bulletin* **1987**, *22*, 631-639, https://doi.org/10.1016/0025-5408(87)90112-7.
11. Wu, W.; Mohamed, A.; Whitacre, J.F. Microwave synthesized $NaTi_2(PO_4)_3$ as an Aqueous Sodium- Ion Negative Electrode. *J. Electrochem. Soc*.2013,*160*, A497-A504. *https://doi.org/10.1007/s40820-019-0273-1*
12. *Pang, G.;* Yuan, C.; Nie, P.; Ding, B.; Zhu, J.; Zhang, X. Synthesis of NASICON-type structured NaTi2(PO4)3–graphene nanocomposite as an anode for aqueous rechargeable Na-ion batteries. *Nanoscale* **2014**, *6*, 6328-6334,https://doi.org/10.1039/C3NR06730K.
13. Qu, Q.T.; Liu, L.L.; Wu, Y.P.; Holze, R. Electrochemical behavior of V2O5·0.6H2O nanoribbons in neutral aqueous

electrolyte solution. *Electrochimica Acta* **2013**, *96*, 8-12,https://doi.org/10.1016/j.electacta.2013.02.078.

14. Qin, H.; Song, Z.P.; Zhan, H.; Zhou, Y.H. Aqueous rechargeable alkali-ion batteries with polyimide anode. *Journal of Power Sources* **2014**, *249*, 367-372,https://doi.org/10.1016/j.jpowsour.2013.10.091.

15. Pasta, M.; Wessells, C.D.; Liu, N.; Nelson, J.; McDowell, M.T.; Huggins, R.A.; Toney, M.F.; Cui, Y. Full open-framework batteries for stationary energy storage. *Nature Communications* **2014**, *5*, https://doi.org/10.1038/ncomms4007.

16. González, J.R.; Alcántara, R.; Nacimiento, F.; Ortiz, G.F.; Tirado, J.L. Microstructure of the epitaxial film of anatase nanotubes obtained at high voltage and the mechanism of its electrochemical reaction with sodium. *CrystEngComm***2014**, *16*, 4602-4609,https://doi.org/10.1039/C4CE00272E.

17. Ladislav, K.; Martin, K.; Marketa, Z.; Ivan, E.; Volker, L.; Reinhard, N.; Michael, G. Lithium Storage in Nanostructured TiO_2 Made by Hydrothermal Growth. *Chem. Mater.***2004,***16*, 477−485. https://doi.org/10.1021/cm035046g

18. Wagemaker, M.; Kentgens, A.P.M.; Mulder, F.M. Equilibrium lithium transport between nanocrystalline phases in intercalated TiO2 anatase. *Nature* **2002**, *418*, 397-399,https://doi.org/10.1038/nature00901.

19. Kavan, L.; Grätzel, M.; Gilbert, S.E.; Klemenz, C.; Scheel, H.J. Electrochemical and Photoelectrochemical Investigation of single-Crystal Anatase. *J. Am. Chem. Soc.* **1996**, *118*, 6716−6723. https://doi.org/10.1021/ja954172l

20. Hu, Y-S.; Kienle, L.; Guo, Y-G.; Maier, J. High Lithium Electroactivity of Nanometer- Sized Rutile TiO_2**. *Adv. Mater.***2006,***18*, 1421−1426, https://doi.org/10.1002/adma.200502723.

21. Dambournet, D.; Belharouak, I.; Amine, K. Tailored Preparation Methods of TiO_2 Anatase, Rutile, Brookite: Mechanism of Formation and Electrochemical Properties. *Chem. Mater.***2010**, *22*, 1173−1179. https://doi.org/10.1021/cm902613h

22. Gonzalez, J.R.; Ricardo, A.; F, Nacimiento.; G.F, Ortiz.; Jose, L. Tirado. Self- Organized, Anatase, Double-Walled Nanotubes Prepared by AnodiZation under Voltage Ramp as Negative Electrode for Aqueous Sodium-Ion Batteries. *Journal of the Electrochemical Society***2015**, *162*, A3007-A3012, https://doi.org/10.1149/2.0021502jes.

23. Kim, K-T.; Ghulam, A.; Chung, K.Y.; Yoon§, C.S.; Yashiro, H.; Sun, Y-K.; Lu, J.; Amine, K.; Myung, S-T. Anatase Titania Nanorods as an Intercalation Anode Material for Rechargeable Sodium Batteries. *Nano Lett.* **2014**, *14*, 416−422. https://doi.org/10.1021/nl402747x

24. Yogendra, K, Vinod Kumar, V: Dipak Kumar, D. Synthesis of perovskite type $NdFeO_3$ nanoparticles and used as electrochemical sensor for detection of paraetamol, *Letters in Applied NanoBioScience* **2020**, 9, 866 – 869. https://doi.org/10.33263/LIANBS91.866869.

25. Dahryn Trivedi,D: Mahendra Kumar, T:, Alice, B: Gopal,N: Jana, S. Characterization of the biofield energy treated aluminium using PSA, PXRD, and TGA/DTG analytical techniques. *Letters in Applied NanoBioScience* **2019**, 8, 637 – 642. https://doi.org/10.33263/LIANBS83.643648

26. Liming, W.; Dominic, B.;Daniel, B.; Stefano, P. Nanocrystalline TiO_2 (B) as Anode Material for Sodium-Ion Batteries. *Journal of the Electrochemical Society* **2015**, *162*, A3052-A3058, https://doi.org/10.1149/2.0091502jes.

27. Manickam, M.; Singh, P.; Issa, T.B.; Thurgate, S. Electrochemical behavior of anatase TiO2 in aqueous lithium hydroxide electrolyte. *Journal of Applied Electrochemistry* **2006**, *36*, 599-602,https://doi.org/10.1007/s10800-005-9112-9.

28. Lyon, L.A.; Hupp, J.T. Energetics of the Nanocrystalline Titanium Dioxide/ Aqueous Solution Interface: Approximate Conduction Band Edge Variations between H0= -10 and H- = +26. *J. Phys.Chem.* **1999**, *B 103*, 4623-4628. https://doi.org/10.1021/jp9908404

29. Lyon, L.A.; Hupp, J.T. Energetics of semiconductor Electrode/Solution Interfaces: EQCM Evidence for Charge-Compensating Cation adsorption and Intercalation during Accumulation Layer Formation in the Titanium Dioxide/Acetonitrile System. *J. Phys. Chem*. **1995**, *99*, 15718-15720. https://doi.org/10.1021/j100043a005

6. ACKNOWLEDGEMENTS

The authors gratefully acknowledge the financial support from the Department of Science and Technology, (SERB-DST), Project No.ECR/2016/000644, Government of India. Authors wish to thank the Management, GITAM (Deemed to be University), Bengaluru for the support and encouragement.